Available online at www.sciencedirect.com
SCIENCE DIRECT®
ELSEVIER
Colloids and Surfaces A: Physicochem. Eng. Aspects 270–271 (2005) 270–276
COLLOIDS AND SURFACES A
www.elsevier.com/locate/colsurfa

Doublet dynamics of magnetizable particles under frequency modulated rotating fields

P. Domínguez-García [a,*], Sonia Melle [a,b], Oscar G. Calderón [b], M.A. Rubio [a]

[a] *Dpto. Física Fundamental, UNED, Senda del Rey s/n, Madrid 28040, Spain*
[b] *Dpto. Optica, Universidad Complutense de Madrid, C. Universitaria s/n, Madrid 28040, Spain*

Available online 15 July 2005

Abstract

We study experimentally the dynamics of an isolated pair of paramagnetic micro-particles when applying rotating and frequency modulated magnetic fields. In the case of purely rotating field, the inter-particle distance performs radial oscillations above a given threshold. The oscillation threshold depends on the viscosity and the amplitude of the magnetic field. When the data are represented in terms of the relative distance to the critical Mason number all curves collapse nicely. The master curve obtained shows the same features that are obtained in numerical simulations. For frequency modulated rotating fields, complex and irregular dynamics is obtained. This dynamics is again in qualitative agreement with numerical simulations.

Keywords: Doublet dynamics; Paramagnetic micro-particles; Modulated frequency rotating fields

1. Introduction

Magnetic particles are important in many areas of science and technology. In the last decades, there has been an increasing interest on model particle systems in which particles move freely suspended in a medium where the magnetic interactions play an important role concerning micro-structure evolution and dynamical behaviour. These systems include ferrofluids (colloids of ferromagnetic nanoparticles dispersed in carrier liquids) [1], magneto-rheological fluids (colloids of magnetic or magnetizable micro-particles immersed in a non-magnetic fluid) [2], and the so-called magnetic holes (non-magnetic micro-particles immersed in a ferrofluid) [3].

Previous experimental work in systems subject to external rotating magnetic fields [4–11] demonstrate that these systems may show a very rich dynamics depending on parameters, such as the amplitude and frequency of the rotating field, and the viscosity of the carrier fluid. The work in Ref. [4] is particularly relevant in this context, because it deals with the dynamics of a system of magnetic holes. This system is formed by a pair of spherical polystyrene particles with diameter around 10–100 μm immersed in a ferrofluid made of a colloidal suspension of magnetite particles (diameter ~ 0.01 μm) dispersed in kerosene.

Helgesen et al. find two different rotating regimes depending on the value of the rotating frequency being below or above a threshold frequency [4]. At low frequencies, the two particles rotate synchronously with the field, whereas above the frequency threshold the pair is not able to follow the field, due to the viscous friction, so its phase lag increases with time until it reaches the value $\pi/2$. Beyond this point, the magnetic torque reverses sign, forcing the pair to rotate backwards. This continues until the field “catches up” with the pair and a new cycle of forward and backward rotation takes place. Furthermore, in this asynchronous rotation regime, an additional radial oscillation of the pair is observed in which the particles separate a certain distance each time the axis between the particles rotates opposite to the field.

Numerical simulations of systems made of pairs of magnetic particles or magnetic holes have shown similar behaviour [5]. Later experimental work [6] on pairs of magnetosoft millimeter-size particles immersed in highly viscous fluids has focused on the influence of particle

* Corresponding author.
E-mail address: pdominguez@bec.uned.es (P. Domínguez-García).

0927-7757/$ – see front matter
doi:10.1016/j.colsurfa.2005.06.012

surface conditions in the pair dynamics. Results concerning more complex systems of up to seven particles were briefly reviewed in Ref. [7]. Different rotational modes were found depending on the rotating field frequency. At very high frequencies, these modes became extremely complicated and chaotic states were found.

Experimental studies regarding the dynamics of many-particle systems under rotating magnetic fields have been recently reported in magneto-rheological suspensions [8–11]. In these systems, the particles form chains that rotate with the field but lag behind with a retardation angle that depends on the experimental conditions. In those works, we were able to show that the dynamics of the field-induced structures under rotating fields is governed by the ratio of viscous to magnetic forces. A dimensionless parameter that measures the ratio of these two forces is the so-called Mason number, which has been defined as

$$\mathrm{Ma} = \frac{12^2 \eta 2\pi f}{\mu_0 M^2} \qquad (1)$$

where η is the solvent viscosity, f the frequency of the rotating magnetic field, μ_0 the vacuum magnetic permeability, and M is the particle magnetization. With this definition, a value of Ma close to unity corresponds to the threshold of stability of a particle pair. Consequently, in the case of the many-particle systems, the system dynamics shows a cross-over at $\mathrm{Ma_c} \sim 1$, above which the viscous forces dominate and inhibit the aggregation process.

Here, we report on an experimental study of the dynamics of an isolated pair of superparamagnetic particles under rotating magnetic fields. Following previous work [4–7], we analyse the behaviour of the doublet with the rotating field frequency. In particular, we focus on general features of the system dynamical behaviour close to the threshold frequency for the radial oscillations. We also study the doublet dynamics when the external rotating field is itself frequency modulated. In this case, very complex and irregular behaviour is obtained. The results in both cases are also compared to numerical simulations, obtaining qualitative agreement.

2. Experimental and numerical methods

2.1. Experimental procedure

We start from suspensions of monodisperse superparamagnetic particles in water supplied by *microParticles GmbH*. The particles are made of a polystyrene matrix that contains a certain amount of magnetite nanosized particles. The average particle diameter is 8 μm. The viscosity of the carrier fluid can be varied by adding glycerol to the suspension. The suspension sample is confined between two quartz windows separated by a spacer that sets the gap between the windows to 100 μm. A circulation thermostatic bath keeps the temperature during the experiments set at $T = 282$ K.

When a magnetic field $\vec{H}$ is applied, the particles in the suspension acquire a dipole moment $\vec{m} = (4\pi/3)a^3\vec{M}$, where $\vec{M} = \chi\vec{H}$ and a are the particle magnetization and the radius, respectively, and χ is the particle magnetic susceptibility. Then, due to dipolar interactions, the particles aggregate to form chains aligned in the field direction.

The experimental setup is shown in Fig. 1 that has been thoroughly described in Ref. [9]. The left panel displays the system used to generate the magnetic field which consists of two orthogonal pairs of coils driven by two arbitrary programmable function generators. In order to achieve a rotating magnetic field, we program in the function generators sinusoidal signals with a phase difference of $\pi/2$.

The right panel in Fig. 1 displays the video-microscopy setup used to record the images. Below our sample, there is a long working distance microscope (Navitar), with zoom capabilities, attached to a digital CCD camera. The images are recorded every 50 ms and subsequently analysed in the computer to calculate the distance between the centres of the two particles. Fig. 2 displays the process of image computer analysis. On the top part, the images of the former particles are presented, whereas in the lower part, there are the processed images.

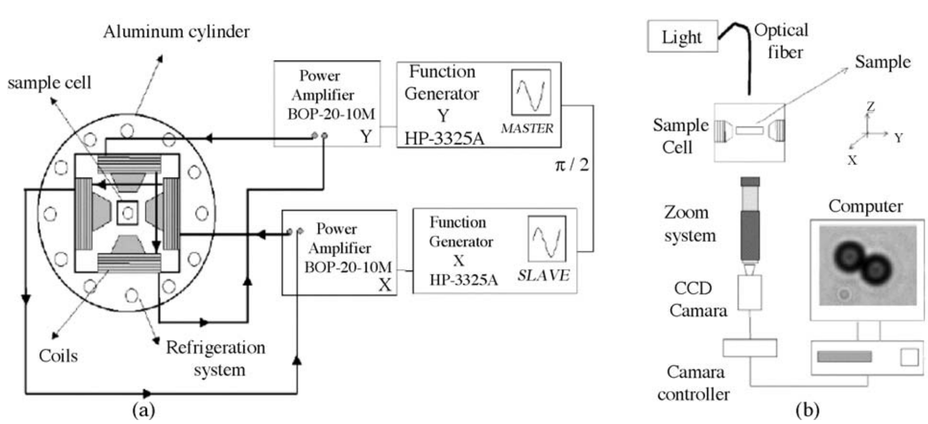

Fig. 1. Experimental setup used to (a) generate the magnetic fields in the plane of the sample $(X - Y)$ and (b) to record the images.

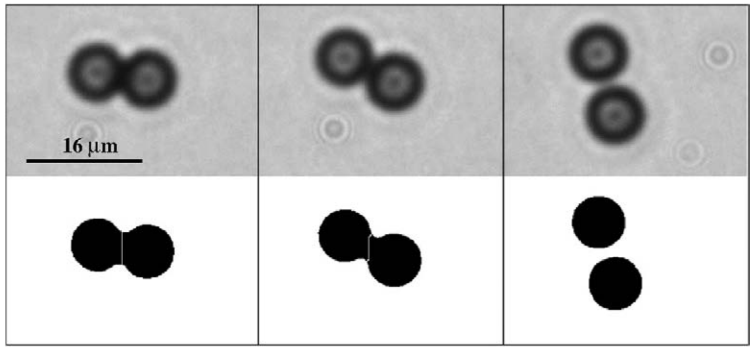

Fig. 2. Doublet images analysis.

2.2. Theoretical model

The model used in the numerical simulations considers the evolution equations of a pair of spherical superparamagnetic particles suspended in a fluid of viscosity η and subject to a rotating magnetic field of frequency f. Consequently, the model ingredients are Stokes friction of the particles with the solvent, magnetic dipole–dipole interaction, and exclude-volume force to keep particles from overlapping [12,13] (for more details about the model, see Ref. [14]).

The dimensionless equations for the distance between particle centres, in units of the particle diameter, R, and the angle of the pair orientation, φ, are given by:

$$\frac{\mathrm{d}R}{\mathrm{d}\tau} = \frac{2}{R^4}[1 - 3\cos^2(2\pi f t_s \tau - \varphi)] + 2A\exp[-B(R-1)] \qquad (2)$$

$$\frac{\mathrm{d}\varphi}{\mathrm{d}\tau} = \frac{2}{R^5}\sin 2(2\pi f t_s \tau - \varphi) \qquad (3)$$

where the temporal coordinate has been made dimensionless by using as typical time scale $t_s \equiv 12^2\eta/(\mu_0 M^2)$, i.e., $\tau \equiv t/t_s$. This time scale, t_s, yields a dimensionless field rotation frequency equal to the Mason number $2\pi f t_s \equiv \mathrm{Ma}$, i.e., to the ratio of the viscous to magnetic forces. That means that in this model, the dynamics of the particle pair depends only on the Mason number. In the simulations here reported, the values given to the constants of the excluded volume force are $A = 2$ and $B = 10$ (see last term of Eq. (2)). In Eqs. (2) and (3), we have neglected the inertia term, which is reasonable for slow motion of particles of the size here considered, and the random thermal fluctuations, which again is a reasonable approximation when the dipolar interaction energy is much higher than $k_B T$.

3. Results

Typical experimental results for the doublet dynamics under a purely rotating field are shown in Fig. 3 that correspond to a doublet immersed in a 30% glycerol in water solution under a magnetic field with amplitude 7.44 kA/m. These graphs are quite similar to those reported for different but closely related systems [4–6].

In Fig. 3(a), we illustrate the temporal evolution of the distance between particle borders, $D(t)$, for three different frequencies of the rotating field. Two different regimes appear depending on the field frequency. For frequencies smaller than a critical frequency (in this particular case, $f_c = 0.25$ Hz), the two particles are always in contact during rotation, i.e., the inter-particle distance D shows very small fluctuations. For high frequencies, above this critical frequency, the distance between particle borders exhibits radial oscillations whose amplitude decreases when increasing the rotating field frequency. This is better appreciated in Fig. 3(b) where we plot the average inter-particle distance, D_{mean}, as a function of the rotating field frequency.

Fig. 3(c) shows the variation of the doublet rotation frequency with the field frequency. The doublet rotation frequency can be obtained from the temporal evolution of the angular coordinate in two methods: as the inverse of the time, the doublet needs to make a 2π rotation or from the position of the peak of its Fourier transform. Both methods give undistinguishable results. The results in Fig. 3(c) can be interpreted as follows. Below the critical frequency for radial oscillations, the doublet rotates synchronously with the applied field. Slightly above the critical frequency, the doublet rotation frequency shows a decreasing trend, due to the large radial oscillations that lower the magnetic interaction between the particles and slow down the rotation. At larger values of the field frequency, the amplitude of the radial oscillations becomes very small and the doublet is able to rotate faster.

In Fig. 3(d), the dots represent the frequency of the radial oscillations as a function of field frequency. Note that the frequency of the radial oscillations can be defined only above the critical frequency. The frequency of the radial oscillations is an increasing function that can be fully explained in terms of the difference between the field rotation frequency and the doublet rotation frequency. Actually, the cause the radial oscillation appears because the particles repel each other when the field is orthogonal to the doublet axis. More-

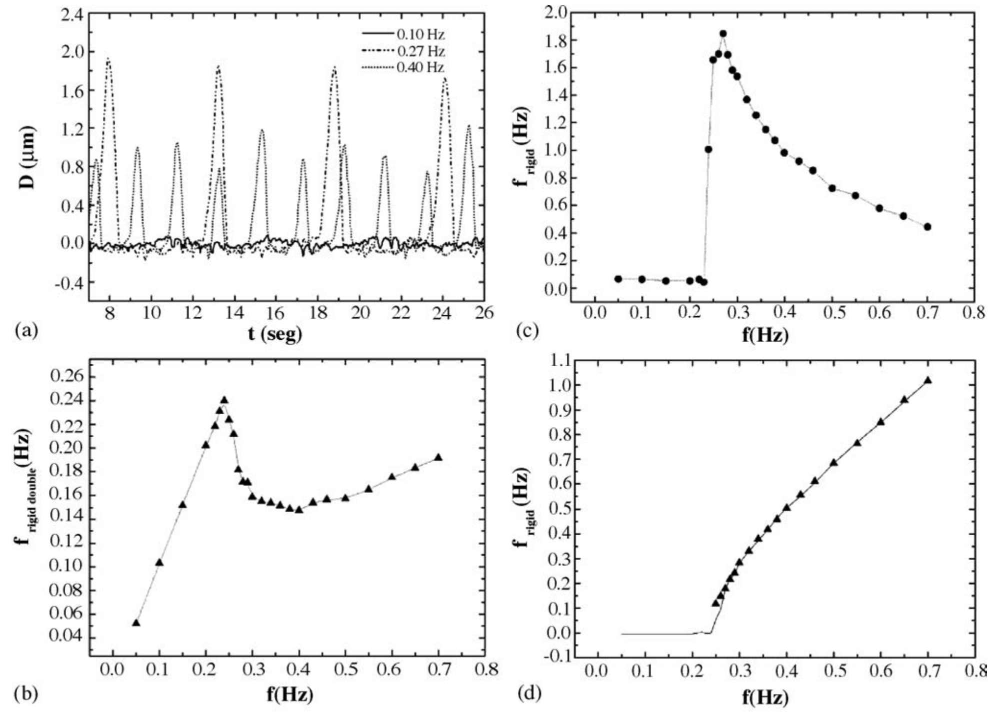

Fig. 3. (a) Example of experimental temporal evolution of distance between particle borders $D(t)$, (b) average distance between particle borders, (c) frequency of the radial oscillations, and (d) doublet rotation frequency as a function of the rotating field frequency f, for a 30% glycerol in water suspension and a magnetic field amplitude of 7.44 kA/m.

over, Fig. 3(c) shows that above the critical frequency the field rotates faster than the doublet. This makes that the field-doublet orthogonality condition is fulfilled twice during the time t_{ft} needed for the field to gain a full turn over the doublet. During that time, the doublet would make $n = t_{ft} f_{\text{rigid doublet}}$ turns, while the field would make $n + 1 = t_{ft} f$ turns. Therefore, $t_{ft} = (f - f_{\text{rigid doublet}})^{-1}$. Now, in the time t_{ft} the doublet makes two radial oscillations and, consequently, the frequency of the radial oscillations is $f_{\text{radial}} = 2(f - f_{\text{rigid doublet}})$. The solid line in Fig. 3(d) represents the results of applying this formula to the data in Fig. 3(c). The agreement is extremely good.

To analyse the interplay between viscous and magnetic forces [10] in the doublet dynamics, we have measured the dependence of the average inter-particle distance on the field frequency for different viscosities and magnetic field strengths. The results are shown in Fig. 4. The behaviour is, in all cases, qualitatively similar to the one shown in Fig. 3(b), but the critical frequency in each curve takes different values depending on the experimental conditions.

According to previous work in many-particle magneto-rheological suspensions [10], the particle dynamics is governed by the Mason number. Thus, it is expected that all curves in Fig. 4 collapse into a single one when plotted against the Mason number. Unfortunately, the magnetization curve of these particles is not available to us. However, a comparison between experimental and simulation results can be made in terms of the behaviour of the average distance between particle borders as a function of the relative distance to the critical value of the Mason number, namely $(\text{Ma} - \text{Ma}_c)/\text{Ma}_c$; in the case of the simulations, $\text{Ma}_c = 1.15$.

This comparison is shown in Fig. 5(a and b). Both the experimental and the simulation curves show the same general features: a levelling off at the lower values of the control parameter, and a possible power-law behaviour, with expo-

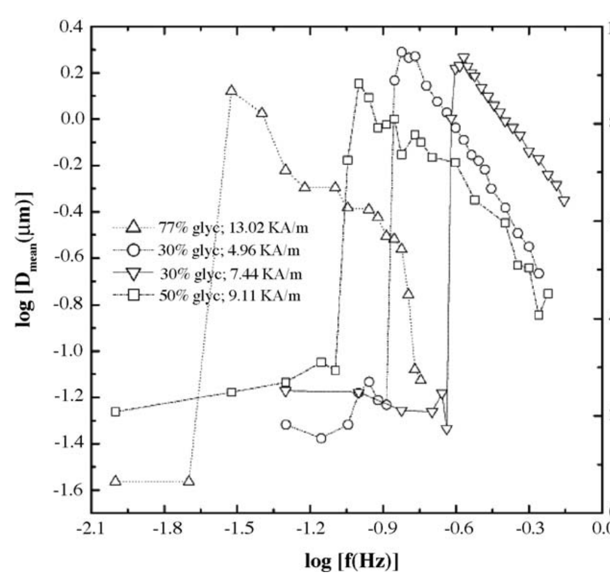

Fig. 4. Logarithmic experimental radial distance between both particle borders as a function of the rotating field frequency for different experimental conditions.

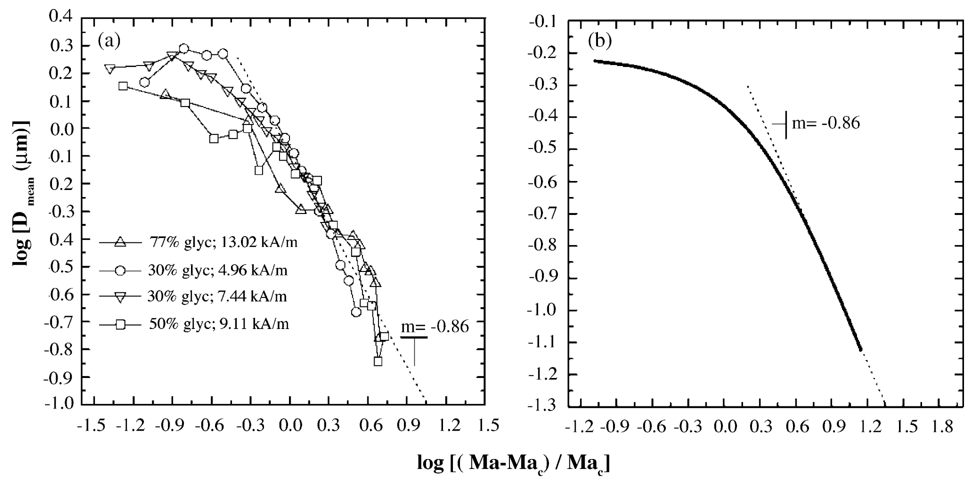

Fig. 5. Experimental (a) and numerical (b) radial distance between particle borders as a function of $(\mathrm{Ma}-\mathrm{Ma_c})/\mathrm{Ma_c}$.

nent ~ -0.86 at large values of $(\mathrm{Ma}-\mathrm{Ma_c})/\mathrm{Ma_c}$. The dashed line in Fig. 5 is just a guide for the eye.

The main discrepancy between experiments and simulations appears in the amplitude of the radial oscillation, the experimental values being smaller by a factor slightly larger than 2. Several physical mechanisms may be at work to diminish the amplitude of the radial oscillation. For instance, hydrodynamic interaction of the particles with the lower glass plate (particles are denser than the carrier fluid) adds some extra viscous dissipation which may be thought of as an increase in Ma. This effective increase in Ma would cause a decrease in the amplitude of the radial oscillation according to Fig. 5(a and b). Another possible mechanism is particle–particle hydrodynamics interaction. Once the doublet is formed, lubrication forces oppose the separation motion and this opposition would necessarily lower the amplitude of the radial oscillation.

4. Modulated rotating field frequency

The more complex regime exhibited by the doublet corresponds to the radial oscillations, where the inter-particle distance presents a periodic behaviour. However, a perturbation of the rotating field frequency can change dramatically the doublet motion. To illustrate this phenomenon, we perturb the doublet dynamics by introducing a periodic modulation of the rotating field frequency f, i.e.,

$$f \rightarrow f = f_0 + \Delta\Omega \sin(2\pi\Omega t) \quad (4)$$

where f_0 is the average rotating field frequency, $\Delta\Omega$ the amplitude of the modulation, and Ω is the modulation frequency. With this type of perturbation, we look for some kind of resonant behaviour when the modulation frequency Ω approaches the value of the frequency of the radial oscillations with no modulation, i.e., when Ω is close to $f_{\mathrm{radial}}(f_0)$.

In the experiments, we used $H = 4.96$ kA/m and 30% glycerol in water solution as carrier fluid. The critical frequency for the radial oscillations is then $f_c = 0.13$ Hz. We have used an average rotating field frequency approximately double than the critical one, i.e., $f_0 = 0.23$ Hz, and a small modulation amplitude $\Delta\Omega = 0.01$ Hz. That means that the instantaneous field frequency $f(t)$ is well above the critical frequency at all times. The corresponding frequency of the radial oscillations without modulation at f_0 is $f_{\mathrm{radial}}(f_0) = 0.3$ Hz.

We have performed numerical simulation by means of Eqs. (2) and (3) and taking $\mathrm{Ma}(t) = 2\pi t_s f(t)$. The critical Mason number is $\mathrm{Ma_c} \cong 1.15$. Then, we use an average dimensionless rotating frequency, $\mathrm{Ma_0}$, double than the critical one, i.e., $\mathrm{Ma_0} = 2.3$, and a dimensionless modulation amplitude of 0.01.

In the analysis of the doublet dynamics as a function of the modulation frequency Ω, we found several different dynamical regimes that are plotted in Fig. 6, where left panels correspond to experiments and right panels to simulations, respectively. At very small values of Ω, the doublet behaves as in the case without modulation, i.e., the radial periodic oscillations are present with the expected frequency $f_{\mathrm{radial}}(f_0)$ (see Fig. 6 (top)). However, at intermediate values of Ω – but lower than $f_{\mathrm{radial}}(f_0)$ – the pair motion presents a very irregular behaviour. In particular (see Fig. 6 (middle)), at certain modulation frequencies, big amplitude oscillations occur, which separate both particles and keep them apart during long time periods (tens of seconds).

These large oscillations yield large values of the average inter-particle distance, as shown in Fig. 7(a and b), where the average inter-particle distance is plotted as a function of the modulation frequency for experiments and simulations, respectively. We observe peaks in the central region of modulation frequencies which correspond to the big oscillations mentioned above.

Both curves in Fig. 7(a and b) show pronounced maxima at a modulation frequency $\Omega \sim 0.23$ Hz. Note that this value

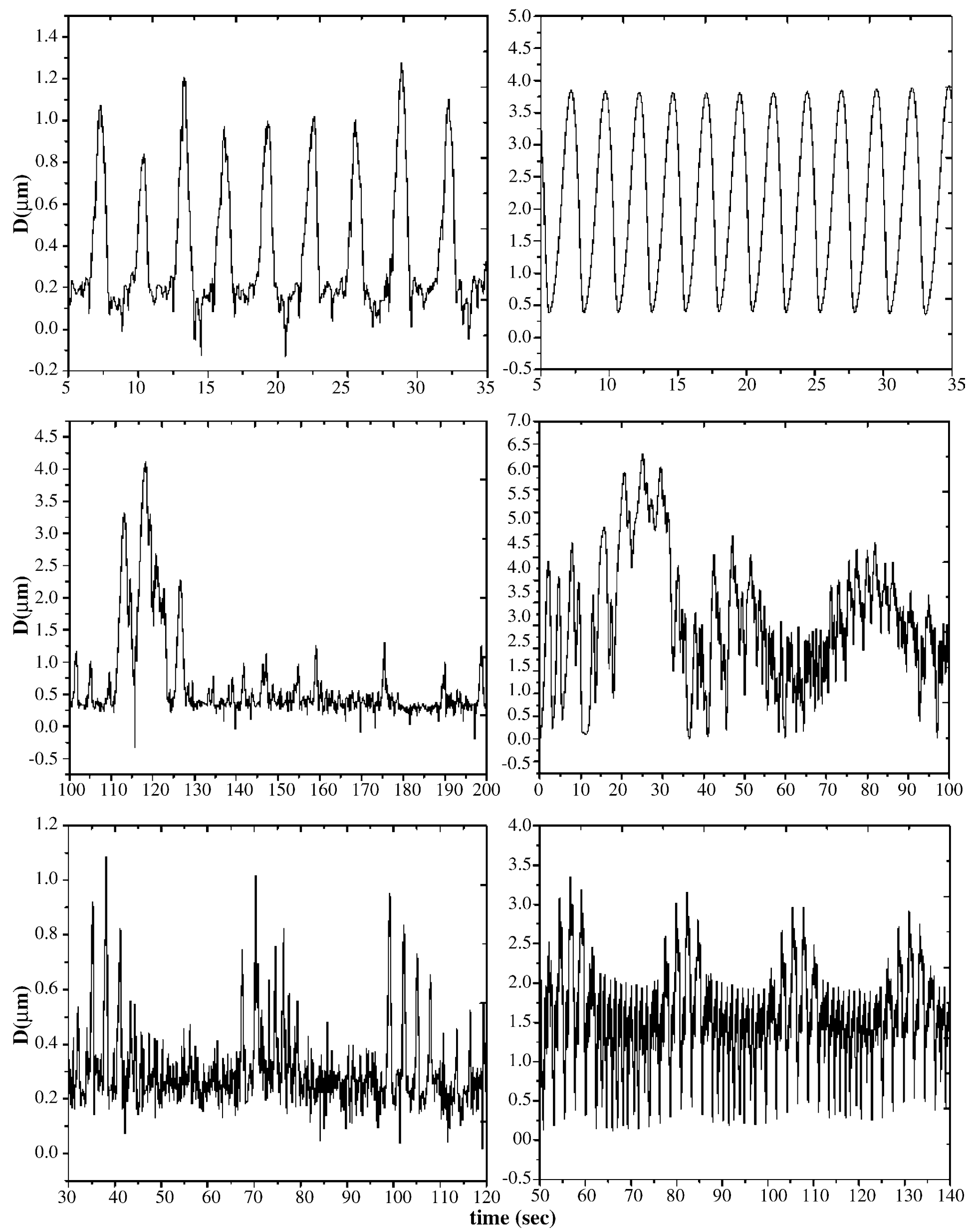

Fig. 6. Experimental (left) and theoretical (right) temporal evolution of inter-particle distance; (top) $\Omega = 0.01$ Hz, (middle) $\Omega = 0.21$ Hz, and (bottom) $\Omega = 0.33$ Hz.

coincides with the average rotating field frequency f_0. Note that when $\Omega = f_0$ the field rotation is not uniform in time but is certainly periodic with frequency Ω. Another peak can be appreciated in Fig. 7(a and b) at $\Omega \sim 0.15$ Hz. This is close to the critical frequency for the radial oscillations $f_c = 0.13$ Hz.

When the modulation frequency Ω is close to the frequency of the radial oscillation without modulation $f_{radial}(f_0)$, the doublet motion becomes more regular, as shown in Fig. 6 (bottom). In particular, the graph corresponding to the numerical results shows a signal with well-defined frequencies close to $f_{radial}(f_0)$ and $2f_{radial}(f_0)$. This more regular signal is accompanied by a decrease of the average distance between particle borders, even below the one corresponding to the case without modulation, as can be seen in the region of high frequencies $\Omega \sim 0.4$ Hz in Fig. 7.

Hence, we may say that the dynamical behaviour obtained in the numerical simulations is in qualitative agreement with the experimental one. However, also in the case of the frequency modulated magnetic field, the amplitude of the radial oscillations in the experiments is consistently smaller than in the simulations. It is appealing to conjecture that the same explanation suggested in the case of the non-frequency modulated rotating field may be likely applied.

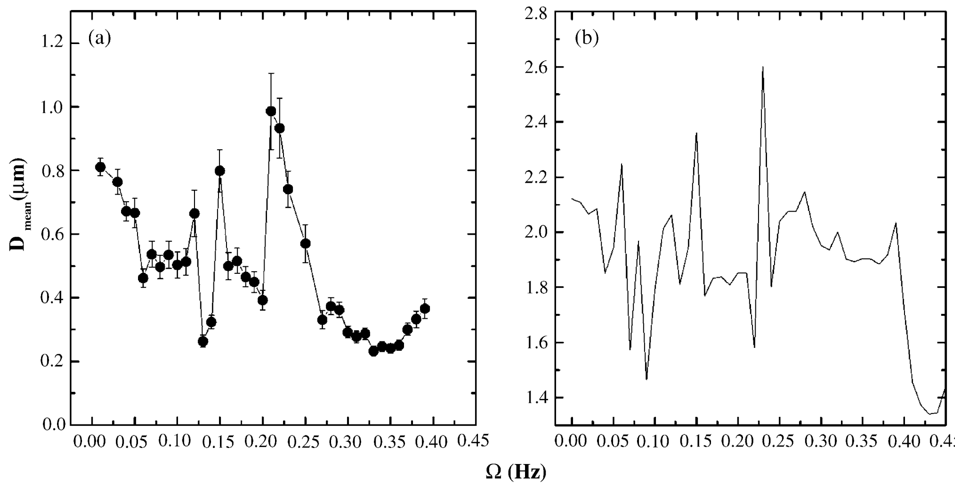

Fig. 7. Experimental (a) and theoretical (b) values of mean radial distance between centres in units of the particle diameter as a function of the modulation frequency Ω.

5. Conclusions

We have studied experimentally the dynamics of an isolated pair of superparamagnetic micro-particles under an external rotating magnetic field. We have found two different rotation regimes: rigid-like synchronous rotation and radial oscillation asynchronous rotation. In these regimes, the dynamics of the doublet may be analysed in terms of a single control parameter: the Mason number, which represents the ratio between viscous and magnetic forces. When plotted versus the relative distance to the critical Mason number for radial oscillations, the curves corresponding to the amplitude of the radial oscillations for different field amplitudes and fluid viscosities collapse onto a single master curve.

When the rotating field frequency is itself frequency modulated, complex and irregular dynamics is obtained. In particular, we observe big amplitude oscillations which separate both particles and keep them far away from each other during a long time. When we modulate the rotating field frequency with a frequency close to the expected frequency of the radial oscillations without modulation, the doublet motion becomes more regular and the average inter-particle border distance decreases.

Both in the case of purely rotating field and in the frequency modulated field, the numerical simulations show qualitative agreement with the experimental findings. However, the numerical simulations yield systematically higher radial oscillation amplitude. Possible explanations for this fact are the existence of hydrodynamic interaction between the particles and the bottom glass wall and/or among themselves. This issue clearly deserves further investigation.

Acknowledgments

We are grateful to Julia C. Gómez-Sáez for the correction of the English version of the manuscript. P. Domínguez-García has been supported by an F.P.I. fellowship from M.E.C. This research has been supported by M.E.C. under Project No. BFM2001-0297.

References

[1] J.C. Bacri, A. Cebers, R. Perzynsky, Phys. Rev. Lett. 72 (1994) 2705.
[2] M. Fermigier, A.P. Gast, J. Colloid Interface Sci. 154 (1992) 522.
[3] A.T. Skjeltorp, Phys. Rev. Lett. 51 (1983) 2306.
[4] G. Helgesen, P. Pieranski, A.T. Skjeltorp, Phys. Rev. A 42 (1990) 7271.
[5] B.E. Kashevsky, A.L. Novikova, Magnetohydrodynamics 25 (1989) 304.
[6] B.E. Kashevsky, V.A. Kuzmin, J. Phys. D: Appl. Phys. 29 (1996) 2579.
[7] P. Meakin, A.T. Skjeltorp, Appl. Phys. 42 (1993) 1.
[8] S. Melle, G.G. Fuller, M.A. Rubio, Phys. Rev. E 61 (2000) 4111.
[9] S. Melle, O.G. Calderón, G.G. Fuller, M.A. Rubio, J. Non-Newtonian Fluid Mech. 102 (2002) 135.
[10] S. Melle, O.G. Calderón, G.G. Fuller, M.A. Rubio, J. Colloid Interface Sci. 247 (1) (2002) 200.
[11] S. Melle, O.G. Calderón, G.G. Fuller, M.A. Rubio, Phys. Rev. E 68 (2003) 041503.
[12] M. Mohebi, N. Jamasbi, J. Liu, Phys. Rev. E 54 (1996) 5407.
[13] D.J. Klingenberg, F. van Swol, C.F. Zukovski, J. Chem. Phys. 91 (1989) 7888.
[14] O.G. Calderón, S. Melle, J. Phys. D: Appl. Phys. 35 (2002) 2492.